



# Impacts of Zirconium Carbide Incorporated Magnesium Alloy Nanocomposite on Wear Properties

Pandian Rajendiran<sup>1\*</sup> and Vinayagam Mohanavel<sup>2</sup>

<sup>1</sup>Department of Mechanical Engineering, Bharath Institute of Higher Education and Research, Tambaram, Selaiyur, Chennai, TN, India

<sup>2</sup>Centre for Materials Engineering and Regenerative Medicine, Bharath Institute of Higher Education and Research, Tambaram, Selaiyur, Chennai, TN, India

Received: 08.08.2024 Accepted: 16.09.2024 Published: 30.09.2024

\*pandian138@gmail.com



## ABSTRACT

In the study, zirconium carbide nanoparticle (ZrC-50 nm) incorporated magnesium alloy (AZ61) nanocomposite was prepared by liquid state stir cast process, and its wear properties were evaluated by different load (U), sliding speed (V), and sliding distance (W). The impacts on wear rate (WR) and coefficient of friction (COF) of AZ61 alloy nanocomposite were studied. With the support of a pin-on-disc wear tester, the dry sliding wear characteristics were measured. Moreover, to find the optimum process parameter on minimum WR and better COF characteristics, the L27 orthogonal array utilized U, V, and W as the input factors, and the WR & COF were treated as output responses. Based on the analysis, load was found to be the most dominant input factor that influences the WR and sliding distance was the factor for fixing the COF.

**Keywords:** AZ61; ZrC; Wear rate and coefficient of friction.

## 1. INTRODUCTION

Composites have potential for various engineering and non-engineering applications due to their unique behaviour (Kumar *et al.* 2024). They are classified into two major categories: metal matrix and polymer matrix (Depoures *et al.* 2024). Polymer matrix nanocomposites are utilized in various applications (Venkatesh, 2024). Composites have significantly different physical, chemical, and mechanical properties than their constituent materials. The unique properties of the components that make up these composites, in addition to their comparative volume fractions and configurations within the material system, are what give these composites their distinctive features. Composites may be synthesized to meet definite geometrical, structural, mechanical and aesthetic properties expected in the target material (Egbo, 2021). The usage of composite has been around for a long time. Manufacturing bows, constructing bricks, and a variety of other uses for composite materials support this. With respect to time, the continuous improvement in the field of nanocomposite increased its application. Almost all areas, including sports, medicine, thermal engineering, electrical engineering, aerospace, defence, and many more, are currently using nanocomposite materials (Zhang *et al.* 2023). Applications where weight reduction is a key consideration could make use of metal matrix composites [MMCs] with good stiffness and strength

(Devanathan *et al.* 2024). Robots, fast machinery, and fast rotating shafts for marine and automotive altogether tumble under this group. With better strength and wear resistance MMCs are favoured materials for auto spare manufacturing (Harikrishnan *et al.* 2024).

Noteworthy advances in basic science and technology were accomplished throughout the creation of nano MMCs, including a basic comprehension of composite performance processing of nano MMCs. The experience gained through technology later helped in the fabrication of elevated-temperature intermetallic matrix composites (Rawal, 2001). Magnesium matrix composite materials (MMMCs) are fabricated by reinforcing with ceramic nanoparticles, which is one technique to improve the characteristics of aluminium alloys. When compared to typical alloys, these MMMCs have interesting qualities for the industrial sector, including greater wear resistance, excellent specific resistance, and stronger resistance to thermal deterioration (Suresh and Mohanavel, 2022; Dillikannan *et al.* 2024). Since magnesium and other light metals have a lower density, their use decreases mass, improves efficiency, and satisfies the fundamental criteria for fuel efficiency and vehicle emissions. However, their tribology characteristics are subpar, which restricts their use in the production of tribo-mechanical parts. Utilizing aluminium metal matrix composites is one potential remedy for this issue (Liu *et al.* 2023). Magnesium matrix composite materials are becoming more and more

desirable materials for cutting-edge uses, including aerospace and automotive applications, due to the ability to customize their properties by adding certain reinforcements as sized as micro or nano. They are a very strong candidates for a number of applications when viewed from a scientific and technological perspective due to their properties and relatively low production cost (Aliabadi *et al.* 1990). For elevated temperature usages, nano-sized ZrC particles exhibited better properties, and it is now the top ceramic material (Kumar *et al.* 2023; Chandradass *et al.* 2023). Stir casting is generally recognized as one of the several manufacturing methods available for metal matrix composites and is now used commercially. Its benefits include simplicity, adaptability, and suitability for large-scale production. It is particularly appealing since, in theory, it permits the use of a normal metal processing procedure, lowering the overall cost of the product (Hashim *et al.* 1999; Anjalin *et al.* 2023). One of the most cost-effective ways to process MMC is by stir-casting magnesium alloy-based casting composites.

The expensive cost of making components with complicated shapes has prevented particulate MMCs from being widely used in engineering applications. Jayasathyakawin and Ravichandran (2023) explored the wear behaviour of Mg/3Al matrix composites by the Taguchi process and specific WR and COF are significantly impacted via nano reinforcement weight percentage. The solution to this stir-casting issue may lie in casting technology (Shivalingaiah *et al.* 2022). This work studied the tribological characteristics of nanocomposites via the Taguchi route and reported that wear rate is most influenced by sliding distance. The major significant prompting factors on COF are load and sliding speed as reported earlier by Selvaraj *et al.* (2022) and Wei *et al.* (2013).

## 2. EXPERIMENTAL DETAILS

For this research work, the AZ61 matrix alloy was used as the primary matrix. Nano zirconium carbide (ZrC) particle has been chosen as the reinforcing substance. Magnesium was utilized to improve the wettability of the matrix alloy in ingot form. In order to create the AZ61-15wt% ZrC nanocomposites, stir casting was used. The AZ61 was heated in an electric resistance furnace to a temperature of 800 °C. To maintain its semisolid condition, the liquid metal was then cooled below its liquid temperature. Manual incorporation and mixing were carried out with the warmed ZrC nanoparticles. After reaching a totally liquid condition, the composite melt was further heated to 650 °C, and mechanical blending was done for roughly 4 minutes. To produce AZ61-15wt.% ZrC nanocomposites cast rods, the melt was thoroughly stirred before being placed into a steel mould and allowed to cool. The pin-on-disk device was used for the dry sliding wear test (Fig. 1). The

counter disk's rotating disc was constructed of HRC-65 EN-32 steel.



Fig. 1: Pin on Disc wear tester entire setup.

Table 1. Experimental results

| Exp. No. | U (N) | V (m/s) | W (m) | WR (mm <sup>3</sup> /m) | COF   |
|----------|-------|---------|-------|-------------------------|-------|
| 1        | 3.81  | 2.20    | 350   | 0.003140                | 0.399 |
| 2        | 3.81  | 2.20    | 1450  | 0.003310                | 0.345 |
| 3        | 3.81  | 2.20    | 2050  | 0.002499                | 0.304 |
| 4        | 3.81  | 5.20    | 350   | 0.003154                | 0.333 |
| 5        | 3.81  | 5.20    | 1450  | 0.002365                | 0.330 |
| 6        | 3.81  | 5.20    | 2050  | 0.001873                | 0.319 |
| 7        | 3.81  | 8.20    | 350   | 0.002031                | 0.348 |
| 8        | 3.81  | 8.20    | 1450  | 0.001676                | 0.319 |
| 9        | 3.81  | 8.20    | 2050  | 0.001313                | 0.302 |
| 10       | 11.75 | 2.20    | 350   | 0.004892                | 0.379 |
| 11       | 11.75 | 2.20    | 1450  | 0.003617                | 0.355 |
| 12       | 11.75 | 2.20    | 2050  | 0.002591                | 0.320 |
| 13       | 11.75 | 5.20    | 350   | 0.003594                | 0.370 |
| 14       | 11.75 | 5.20    | 1450  | 0.003658                | 0.343 |
| 15       | 11.75 | 5.20    | 2050  | 0.002237                | 0.325 |
| 16       | 11.75 | 8.20    | 350   | 0.002637                | 0.340 |
| 17       | 11.75 | 8.20    | 1450  | 0.002628                | 0.332 |
| 18       | 11.75 | 8.20    | 2050  | 0.002333                | 0.314 |
| 19       | 17.75 | 2.20    | 350   | 0.005001                | 0.411 |
| 20       | 17.75 | 2.20    | 1450  | 0.003377                | 0.330 |
| 21       | 17.75 | 2.20    | 2050  | 0.002546                | 0.359 |
| 22       | 17.75 | 5.20    | 350   | 0.005587                | 0.405 |
| 23       | 17.75 | 5.20    | 1450  | 0.003333                | 0.366 |
| 24       | 17.75 | 5.20    | 2050  | 0.002007                | 0.359 |
| 25       | 17.75 | 8.20    | 350   | 0.004652                | 0.381 |
| 26       | 17.75 | 8.20    | 1450  | 0.003897                | 0.358 |
| 27       | 17.75 | 8.20    | 2050  | 0.002348                | 0.339 |

The nanocomposite test samples were made as cylinders with 32-mm length and 8-mm diameter. The ASTM G 99-09 standard was followed for conducting the wear tests at room temperature under dry sliding

conditions. For the wear test, a varying sliding distance of 350, 1450, and 2050 m was used along with applied loads of 3.81, 11.75, and 17.75 N at 2.2, 5.2, and 8.2 m/s. By varying the weight, the dry sliding wear rate of the AZ61-15wt% ZrC nanocomposite was determined. Finally, the wear rates (WR) and COF were determined.

**Table 2. Response Table for S/N Ratios for WR**

| Level | U (N) | V (m/s) | W (m) |
|-------|-------|---------|-------|
| 1     | 52.87 | 49.53   | 48.70 |
| 2     | 50.36 | 50.70   | 50.44 |
| 3     | 49.26 | 52.25   | 53.34 |
| Delta | 3.61  | 2.71    | 4.63  |
| Rank  | 2     | 3       | 1     |

**Table 3. Response Table for Means of WR**

| Level | U (N)    | V (m/s)  | W (m)    |
|-------|----------|----------|----------|
| 1     | 0.002373 | 0.003441 | 0.003854 |
| 2     | 0.003132 | 0.003090 | 0.003096 |
| 3     | 0.003639 | 0.002613 | 0.002194 |
| Delta | 0.001265 | 0.000829 | 0.001660 |
| Rank  | 2        | 3        | 1        |

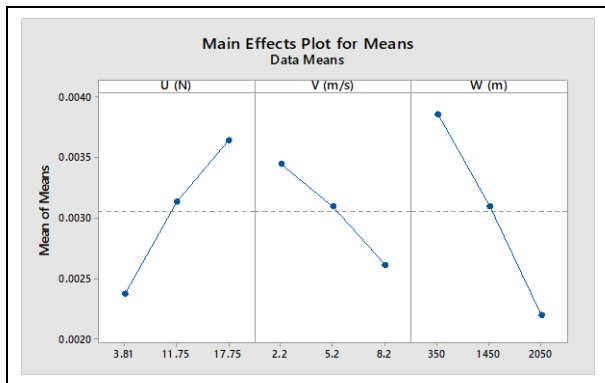


**Fig. 2: Mean plot for WR**

### 3. RESULTS AND DISCUSSION

By experimenting according to the orthogonal array, it was possible to obtain the findings for various parameter combinations. Utilizing specialized design of experiment applications, MINITAB 18 commercial software was used to analyze the measured outcomes. Table 1 displays the average experimental data for WR and COF over two repetitions.

The graphical representations of how process parameters affect WR and COF are shown in Figs. 2-5. The optimal circumstances resulting in the lowest WR and COF were determined by the analysis of these testing findings using the signal-to-noise ratio (S/N). Fig. 2 and Fig. 3 illustrate the ideal conditions for WR and COF.

Thus, the best control factor settings for improved wear resistance were discovered. Table 2 shows the response table for S/N Ratios for WR. Table 3 shows the response table for Means of WR.

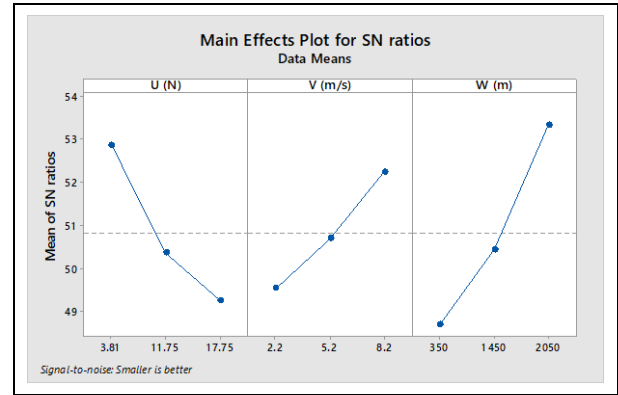


**Fig. 3: S/N ratio plot for WR**

**Table 4. Response Table for S/N Ratios for COF**

| Level | U (N) | V (m/s) | W (m) |
|-------|-------|---------|-------|
| 1     | 9.574 | 9.015   | 8.565 |
| 2     | 9.336 | 9.142   | 9.327 |
| 3     | 8.714 | 9.467   | 9.731 |
| Delta | 0.859 | 0.452   | 1.166 |
| Rank  | 2     | 3       | 1     |

**Table 5. Response Table for Means of COF**

| Level | U (N)  | V (m/s) | W (m)  |
|-------|--------|---------|--------|
| 1     | 0.3332 | 0.3558  | 0.3740 |
| 2     | 0.3420 | 0.3500  | 0.3420 |
| 3     | 0.3676 | 0.3370  | 0.3268 |
| Delta | 0.0343 | 0.0188  | 0.0472 |
| Rank  | 2      | 3       | 1      |

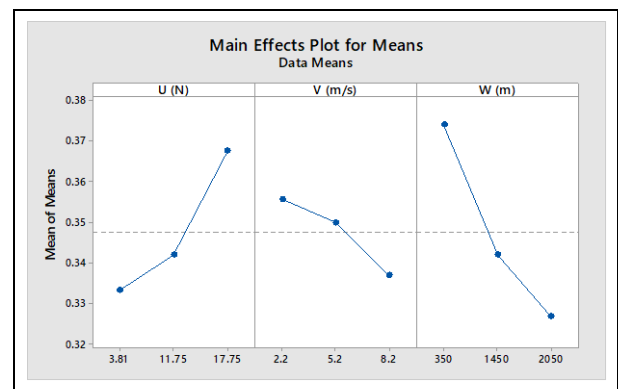


**Fig. 4: Mean plot for COF**

Table 4 represents the response Table for S/N Ratios for COF. Table 5 shows the response table for

Means of COF. ANOVA was performed to examine the effects of the wear parameters that were taken into consideration, specifically the U, V, and W, which have a major impact on the performance measurements. It is possible to determine which independent variable outweighs the others and what proportion that independent variable contributes by using analysis of variance. The ANOVA results for WR and COF for three parameters modified at three levels are shown in Table 6 and Table 7, as well as the interactions between those factors. The last column of Table 6 and Table 7 displays each parameter's percentage contribution (Pr) to the overall variation, demonstrating the extent to which it influenced the outcome. Table 6 shows that the load has the highest influence on WR (23.3%). In light of this, a sliding distance of 4% and sliding speed of 1% are crucial control components to be considered during the wear process. Similarly, Table 7, shows the coefficient of friction and sliding distance contribute 46.3% and load 25%, respectively.

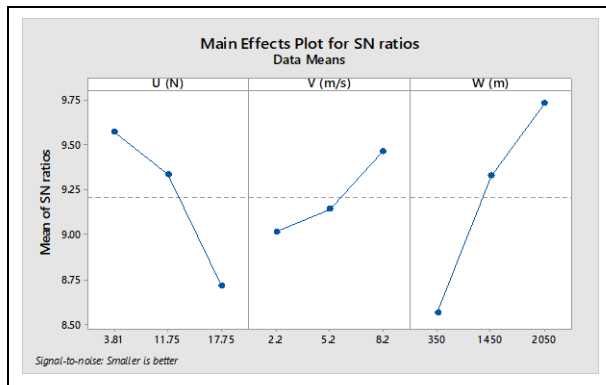


Fig. 5: S/N ratio plot for COF

Table 6. ANOVA for WR

| Source  | DF | Adj SS   | Adj MS   | F-Value | P-Value |
|---------|----|----------|----------|---------|---------|
| U (N)   | 2  | 0.000007 | 0.000004 | 10.42   | 0.001   |
| V (m/s) | 2  | 0.000003 | 0.000002 | 4.44    | 0.025   |
| W (m)   | 2  | 0.000012 | 0.000006 | 17.75   | 0.005   |
| Error   | 20 | 0.000007 | 0.000000 |         |         |
| Total   | 26 | 0.000030 |          |         |         |

Table 7. ANOVA for COF

| Source  | DF | Adj SS   | Adj MS   | F-Value | P-Value |
|---------|----|----------|----------|---------|---------|
| U (N)   | 2  | 0.005727 | 0.002863 | 12.12   | 0.011   |
| V (m/s) | 2  | 0.001665 | 0.000832 | 3.52    | 0.049   |
| W (m)   | 2  | 0.010457 | 0.005228 | 22.13   | 0.013   |
| Error   | 20 | 0.004726 | 0.000236 |         |         |
| Total   | 26 | 0.022575 |          |         |         |

#### 4. CONCLUSION

The following are the findings of the study on Taguchi's method of dry sliding wear test.

- The stir casting process successfully produced AZ61-15wt% ZrC nanocomposite.
- The factors that have the greatest impact on WR are load 23.3%, sliding distance 4% and sliding speed 1%. In case of COF, sliding distance contributes 46.3% and load 25%.
- By providing a barrier between the pin and counter face and using nano-sized ZrC as reinforcement, the wear resistance of composite materials was boosted.

#### FUNDING

This research did not receive any specific grant from public, commercial or non-profit funding agencies.

#### CONFLICTS OF INTEREST

The authors declare that there is no conflict of interest.

#### COPYRIGHT

This article is an open-access article distributed under the terms and conditions of the Creative Commons Attribution (CC BY) license (<http://creativecommons.org/licenses/by/4.0/>).



#### REFERENCES

Aliabadi, M. H., Developments in the Science and Technology of Composite Materials, *Eng Anal. Bound. Elem.*, 7(3), 150 (1990). [https://doi.org/10.1016/0955-7997\(90\)90047-d](https://doi.org/10.1016/0955-7997(90)90047-d)

Anjalin, F. M., Krishnan, A. M., Arunkumar, G., Raju, K., Vivekanandan, M., Somasundaram, S., Thirugnanasambandham, T., Ramaraj, E., Inorganic Adsorption on Thermal Response and Wear Properties of Nanosilicon Nitride-Developed AA6061 Alloy Nanocomposite. *Ads. Sci. Tech.*, 2023, 1-8(2023). <https://doi.org/10.1155/2023/8468644>

Chandradass, J., Thirugnanasambandham, T., Amutha Surabi, M., Baskara Sethupathi, P. and Rajendran, R., Development of Asbestos Free Aramid Fibre based friction lining Material for Automotive Application, *SAE Technical Papers*, (2023). <https://doi.org/10.4271/2023-28-0122>

- Devanathan, C., Dillikannan, D., Akila, P., Kamatchi, R. M., Das, A. D., Karthikeyan, N. and Kaliyaperumal, G., Significance of Hemp Fiber on Mechanical and Thermal Performance of Polypropylene Nanocomposite Developed by Compression Mould Technique, *J. Inst. Eng.*, D (2024). <https://doi.org/10.1007/s40033-024-00687-8>
- Depoures, M. V., Chakravarthy, K. S., Md, J. S., Siva, P. V., Sreenivasa, R. K., Yarram, S. R., Gopal, K., Venkatesh R. and Gautham, M., Sodium Hydroxide Processed Natural Sisal Fiber Made Polypropylene Composite: Characteristics Evaluation, *J. Inst. Eng. (India)*, D (2024). <https://doi.org/10.1007/s40033-024-00761-1>
- Dillikannan, D., Ilavarasan, N., Kamatchi, R. M., Das, A. D., Ammaippan, M., Arunkumar, G. and Kaliyaperumal, G., An Approach of Nano-SiC-Filled Epoxy Nanocomposite Tensile and Flexural Strength Enriched by the Addition of Sisal Fiber, *J. Inst. Eng. (India)*, D (2024). <https://doi.org/10.1007/s40033-024-00680-1>
- Egbo, M. K., A fundamental review on composite materials and some of their applications in biomedical engineering, *J. King Saud Univ. Sci.*, 33(8), 557-568(2021). <https://doi.org/10.1016/j.jksues.2020.07.007>
- Harikrishna, K., Bhowmik, A., Davidson, M. J., Kumar, R., Anqi, A. E., Rajhi, A. A. and Alamri, S., Evaluation of constitutive equations for modeling and characterization of microstructure during hot deformation of sintered Al-Zn-Mg alloy, *J. Mater. Res. Technol.*, 28, 1523-1537 (2024). <https://doi.org/10.1016/j.jmrt.2023.12.050>
- Jayasathyakawin, S. and Ravichandran, M., Fabrication and wear behaviour of Mg-3wt.%Al-x wt. % SiC composites, *Heliyon*, 9(2), 1-15 (2023). <https://doi.org/10.1016/j.heliyon.2023.e13679>
- Kumar, M. V., Lakshmanan, S., Kumar, A., Manivannan, S., Chandramohan, P. and Kaliyaperumal, G., Development of Low-Density Polyethylene Nanocomposite with CNT Fibre Via Injection Moulding: Performance Study, *J. Inst. Eng. (India)*, D.(2024). <https://doi.org/10.1007/s40033-024-00674-z>
- Kumar, T. S., Thankachan, T., Shalini, S., Ćep, R. and Kalita, K., Microstructure, hardness and wear behavior of ZrC particle reinforced AZ31 surface composites synthesized via friction stir processing, *Sci. Rep.*, 13(1), 20089 (2023). <https://doi.org/10.1038/s41598-023-47381-5>
- Liu, B., Yang, J., Zhang, X., Yang, Q., Zhang, J. and Li, X, Development and application of magnesium alloy parts for automotive OEMs: A review, *J. Magnes. Alloy*, 11(1), 15-47 (2023). <https://doi.org/10.1016/j.jma.2022.12.015>
- Rawal, S., Metal-matrix composites for space applications, *JOM*, 53(4), 14-17 (2001). <https://doi.org/10.1007/s11837-001-0139-z>
- Suresh K. S. and Mohanavel, V., An overview assessment on magnesium metal matrix composites, *Mater. Today: Proce.*, 59, 1357-1361 (2022). <https://doi.org/10.1016/j.matpr.2021.12.015>
- Selvaraj, V. K., Jeyanthi, S., Thiyagarajan, R., Senthil Kumar, M., Yuvaraj, L., Ravindran, P., Niveditha, D. M. and Mebremichael, Y. B., Experimental Analysis and Optimization of Tribological Properties of Self-Lubricating Aluminum Hybrid Nanocomposites Using the Taguchi Approach, *Adv. Mater. Sci. Eng.*, 2023(1), 1-3 (2022). <https://doi.org/10.1155/2022/4511140>
- Shivalingaiah, K., Nagarajaiah, V., Selvan, C. P., Kariappa, S. T., Chandrashekarappa, N. G., Lakshmikanthan, A., Manjunath, P. G. C. and Linul, E, Stir Casting Process Analysis and Optimization for Better Properties in Al-MWCNT-GR-Based Hybrid Composites, *Metals*, 12(8), 1-25 (2022). <https://doi.org/10.3390/met12081297>
- Venkatesh, R., Preparation of High-Density Polypropylene Composite Featured with Natural Neem Fiber Through Injection Mould Route, *J. Inst. Eng. (India)*, D, 1-5 (2024). <https://doi.org/10.1007/s40033-024-00706-8>
- Wei, T. Z., Shamsuri, S. R. B., Chang, S. Y., Rashid, M. W. A. nd Ahsan, Q., Effect of sliding velocity on wear behavior of magnesium composite reinforced with SiC and MWCNT, *Procedia Eng.*, 68, 703-709(2013). <https://doi.org/10.1016/j.proeng.2013.12.242>
- Zhang, C., Li, Z., Zhang, J., Tang, H. and Wang, H, Additive manufacturing of magnesium matrix composites: Comprehensive review of recent progress and research perspectives, *J. Magnes. Alloy*, 11(2), 425-461 (2023). <https://doi.org/10.1016/j.jma.2023.02.005>